Journal of Applied Mechanics Vol. 6, pp. 367-375 (August 2003) JSCE

# Large-Scale FE Simulation of Fault Dynamic Rupture with Slip-Weakening Friction Law

Jun Yin*, Mikio Iizuka**, Kazuro Hirahara***, Zhishen Wu****

* Dr. of Eng., Researcher, Research Organization for Information Science and Technology(RIST), 2-2-54 Naka-Meguru, Meguru-ku, Tokyo 153-0061
** Senior researcher, Research Organization for Information Science and Technology(RIST), 2-2-54 Naka-Meguru, Meguru-ku, Tokyo 153-0061
*** Ph.D., Prof., Dept. of Earth and Planetary Sciences, Nagoya University, Furo-cho, Chigusa-ku, Nagoya, 464-8602
**** Dr. of Eng., Prof. Dept. of Urban and Civil Eng., Ibaraki University, Hitachi, 316-8511

A simple slip-weakening friction law, which is presented by a reduction of friction coefficient with the increasing fault slip, is adopted to simulate the fault rupture process at the initial stage of earthquake generation. It is implemented into GeoFEM with Newmark method for dynamic analysis. The fault is modeled by master-slave contact element. A large-scale 3-D simulation of dynamic fault rupture of a part of Northeast Japan area with over 2 million finite element nodes is performed on the Earth Simulator. The attempt of such a large-scale FE simulation has been achieved and the dynamic fault rupture process is presented.

*Key Words: fault rupture, dynamic, slip-weakening friction law, earthquake*

## 1. Introduction

Earthquake, generated on the fault between relative shifting plates, is one of the serious natural disasters which have brought human beings a lot of loss. However, up to now, there is not yet an effective approach to predict the occurrence of earthquake so as to minimize its damage to human society. Currently, advanced observation techniques such as GIS have been able to obtain the plate motion data, from which people could qualitatively predict the earthquake occurrence. But this is far from sufficiency. To get more accurate prediction of future earthquake, a very large-scale and highly accurate simulation is indispensable. Earth Simulator [1], a vectorized parallel supercomputer with computing ability of 40 Tflops for its peak performance, makes such a dream be possible.

The dynamic rupture along a fault at the initial stage of earthquake is a highly complex process involving many factors such as fault geometry, the initial stress field and the constitutive law. The constitutive friction law is one of the important factors of describing the fault rupture because it represents the mechanical characteristics of a fault, though the geometry features also significantly influences the fault rupture process. Therefore, a rational and applicable fault constitutive law for earthquake behavior is required.

Several constitutive laws have been proposed to describe the fault rupture process, among which a slip-weakening law with constant weakening rate and a rate-and-state-dependent friction law [2] are usually adopted. The later one represents a more general form to explain the stick-slip cycle on the fault, which involves slip, slip rate, state variable on the fault and some empirical parameters. It has been applied to a simple one-dimension case by finite difference method [3]. However, the attempt to implement the rate-and-state-dependent friction law into finite element code for 3-dimension simulation has not yet succeeded because it is very difficult to obtain an explicit closed displacement-driven form of due to the highly nonlinear constitutive law and two completely

different time scale during the stick-slip cycle, the stick force accumulation period which is of the order of years physically and fault rupture period which is of the order of only seconds. Alternatively, the slip-weakening friction law is relatively simple with a constant weakening rate. It only deals with the fault rupture process, but not the periodic stick-slip cycle. Therefore, it is relatively easy to be implemented into finite element code for 3-D simulation. To implement the slip-weakening friction law, a master-slave element [4], which is generally used in the simulation of contact problem, is adopted to allow the finite deformation on the fault surface.

Although the ultimate objective of earthquake study is to be able to predict future earthquake occurrence, this paper is to focus on first level study of realizing the 3-D large-scale dynamic fault rupture simulation by using simple slip-weakening friction law.

## 2. Slip-weakening Friction Law

The slip weakening description is originally from the concept of cohesive friction force, and was proposed in numerical models by Andrew [5]. The weakening behavior of friction with the increase of slip has been verified in laboratory experiments [6]. The original slip weakening law assumes that the frictional strength $f_t$ is a function only of the slip $\delta$, where $f_{t0}$ is the yield shear stress, $f_{td}$ is the ultimate frictional kinetic shear stress and $L_d$ is the characteristic slip, also called slip weakening distance, defined as the region where the fracture energy $G_f$ is released (see Fig.1).

$$f_t = \begin{cases} f_{t0}, & \delta = 0^+ \\ f_t(\delta) & \delta < L_d \\ f_{td}, & \delta \geq L_d \end{cases} \qquad (1)$$

However, from the relation of $f_t = \mu f_n$, it can be seen that the $f_{t0}$ is not a fault property which depends on the normal force $f_n$. In the reality, especially in the case of dynamic process, $f_n$ may vary with the time. The friction coefficient $\mu$ is a more objective variable that reflects fault mechanical property. Therefore, in

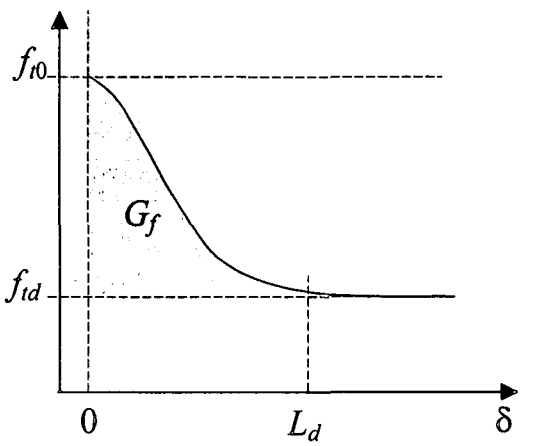


Fig.1 Decrease of frictional force with the increase of slip

the present study, the slip-weakening law in Eq.(1) is modified to the form of the reduction of friction coefficient with the increase of slip. Using a simple linear reduction, the slip weakening friction law can be written as

$$\mu = \begin{cases} \mu_0 - (\mu_0 - \mu_d)\dfrac{\delta}{L_d}, & 0 \leq \delta < L_d \\ \mu_d, & \delta \geq L_d \end{cases} \qquad (2)$$

where $\mu_0$ is initial static friction coefficient, $\mu_d$ is the ultimate dynamic friction coefficient. In this model the fault begins to rupture when the friction force exceeds the yield shear strength $\mu_0 f_n$. The fault friction coefficient then decreases linearly to the dynamic friction coefficient with the slip increasing to $L_d$. The dynamic friction coefficient $\mu_d$ is then retained until $f_t$ becomes less than $\mu_d f_n$, as shown in Fig.2.

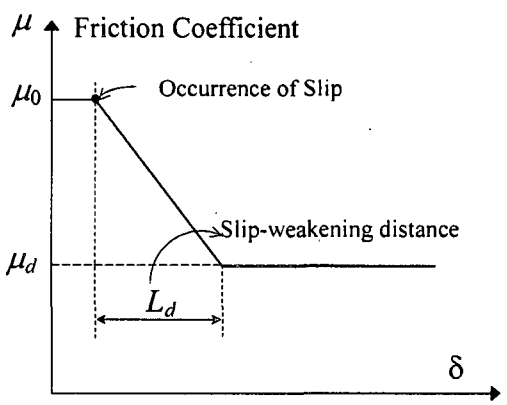


Fig.2 Slip weakening friction law of friction coefficient

## 3. Plasticity Theory of Contact with Friction

### 3.1 Master-Slave Contact Element

To simulate the fault behavior, a master-slave contact element is used in the present study. The master-slave element has been widely applied to the field of contact problem simulation such as metal forming. Fig.3 gives a description of a 3-dimensional master-slave element, which consists of one contact node and 4-node surface.

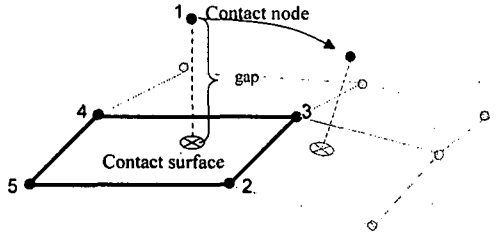


Fig.3 3-D master-slave contact element

Different from the modified joint element, used by Tsuboi and Miura[7], who conducted a finite element analysis of fault rupture based on rock slip experiment, the master-slave element is designed to allow a large deformation simulation. With the deformation, the contact node may move to a new position and make up a new master-slave element with another 4-node surface. Generally, the plate slip during an earthquake, is of the order of centimeters. In the state-of-art of the earthquake simulation, although the mesh discretization is currently only refined to several kilometers due to the computing ability of existing supercomputers, even for Earth Simulator, the much more powerful supercomputers in the future might have the ability to complete more accurate simulation with even more refined mesh in meters. In that case, a several centimeter slip on the fault could no longer be treated as a small deformation. In this sense, the master-slave element is considered promising to deal with the fault rupture behavior. A detailed finite element formulation of master-slave element can be found in [4].

### 3.2 Consistent Tangential Operator On Fault

Based on the penalty method, a frictional contact problem is described following the classic Coulomb plastic law, with a return-mapping algorithm [8]. Considering the slip weakening of the friction coefficient on real fault surface, a new consistent tangent operator is derived.

At a certain time step $t+\Delta t$, the force at one point on the contact surface can be written as

$$ {}^{t+\Delta t}\mathbf{f} = \left|{}^{t+\Delta t}\mathbf{f}_t\right|{}^{t+\Delta t}\mathbf{t} + \left|{}^{t+\Delta t}\mathbf{f}_n\right|{}^{t+\Delta t}\mathbf{n} \tag{3} $$

where ${}^{t+\Delta t}\mathbf{f}_t$ and ${}^{t+\Delta t}\mathbf{f}_n$ are the friction force and contact force. ${}^{t+\Delta t}\mathbf{t}$ is the unit vector of slip direction and ${}^{t+\Delta t}\mathbf{n}$ is the unit vector of contact normal. By differentiating the displacement vector $\mathbf{u}$, Eq.(3) leads

$$ \begin{aligned} \frac{d^{t+\Delta t}\mathbf{f}}{d\mathbf{u}} &= {}^{t+\Delta t}\mathbf{t}\otimes\frac{d\left|{}^{t+\Delta t}\mathbf{f}_t\right|}{d\mathbf{u}} + \left|{}^{t+\Delta t}\mathbf{f}_t\right|\frac{d^{t+\Delta t}\mathbf{t}}{d\mathbf{u}} + {}^{t+\Delta t}\mathbf{n}\otimes\frac{d\left|{}^{t+\Delta t}\mathbf{f}_n\right|}{d\mathbf{u}} \\ &= {}^{t+\Delta t}\mathbf{t}\otimes\frac{d\mu\left|{}^{t+\Delta t}\mathbf{f}_n\right|}{d\mathbf{u}} + \left|{}^{t+\Delta t}\mathbf{f}_t\right|\frac{d^{t+\Delta t}\mathbf{t}}{d\mathbf{u}} + {}^{t+\Delta t}\mathbf{n}\otimes\frac{d\left|{}^{t+\Delta t}\mathbf{f}_n\right|}{d\mathbf{u}} \end{aligned} \tag{4} $$

For simplicity, it is assumed that on contact the master surface is much stiffer than the slave surface, so that the differential of contact normal ${}^{t+\Delta t}\mathbf{n}$ to $d\mathbf{u}$ can be ignored.

In the first term of Eq.(4)'s right side, $d\mu|{}^{t+\Delta t}\mathbf{f}_n|/d\mathbf{u}$ can be further separated to

$$ \frac{d\mu\left|{}^{t+\Delta t}\mathbf{f}_n\right|}{d\mathbf{u}} = \mu\frac{d\left|{}^{t+\Delta t}\mathbf{f}_n\right|}{d\mathbf{u}} + \left|{}^{t+\Delta t}\mathbf{f}_n\right|\frac{d\mu}{d\mathbf{u}} \tag{5} $$

According to the slip-weakening law in Eq.(2), the friction coefficient follows

$$ \mu = \begin{cases} \mu_0 - \dfrac{\mu_0-\mu_d}{L_d}\left|{}^{t+\Delta t}\mathbf{u}_t^p\right| & \left(\left|{}^{t+\Delta t}\mathbf{u}_t^p\right| \le L_d\right) \\ \mu_d & \left(\left|{}^{t+\Delta t}\mathbf{u}_t^p\right| > L_d\right) \end{cases} \tag{6} $$

in which $\left|{}^{t+\Delta t}\mathbf{u}_t^p\right| = \sum_i \sqrt{\Delta u_{t1}^2 + \Delta u_{t2}^2}\,|_i$ denotes the total inelastic length of the slip path history (see Fig.4), where $i$ is the number of iteration.

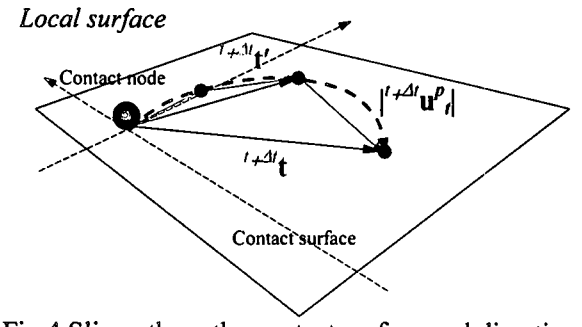


Fig.4 Slip path on the contact surface and direction vectors

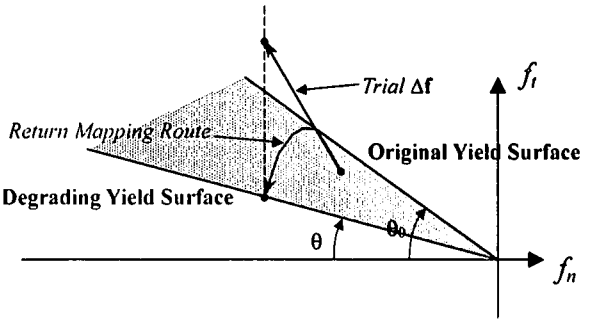


Fig.5 Return mapping procedure to update friction force

The incremental slip at time $t+\Delta t$ can be approximated as $d\left|{}^{t+\Delta t}\mathbf{u}_t^p\right| = \sqrt{\Delta u_{t1}^2 + \Delta u_{t2}^2}$ . By differentiating $d\mathbf{u}$, $d\mu/d\mathbf{u}$ in the second term of Eq.(5) can be derived to

$$\begin{aligned}\frac{d\mu}{d\mathbf{u}} &= -\frac{\mu_0-\mu_d}{L_d}\frac{d\left|{}^{t+\Delta t}\mathbf{u}_t^p\right|}{d\mathbf{u}} \\ &= -\frac{\mu_0-\mu_d}{L_d}\frac{1}{\sqrt{\Delta u_{t1}^2+\Delta u_{t2}^2}}\left[\Delta u_{t1},\Delta u_{t2},0\right]^T \\ &= -\frac{\mu_0-\mu_d}{L_d}{}^{t+\Delta t}\mathbf{t}'\end{aligned} \tag{7}$$

where ${}^{t+\Delta t}\mathbf{t}'$ denotes the unit direction vector of slip increment $[\Delta u_{t1}, \Delta u_{t2}, 0]$. The first term of Eq.(5) can be written to

$$\begin{aligned}\mu\frac{d\left|{}^{t+\Delta t}\mathbf{f}_n\right|}{d\mathbf{u}} &= \mu\frac{d\left|{}^{t+\Delta t}\mathbf{f}_n\right|}{d^{t+\Delta t}\mathbf{f}_n}\cdot\frac{d^{t+\Delta t}\mathbf{f}_n}{d\mathbf{u}} \\ &= \mu\,{}^{t+\Delta t}\mathbf{n}\cdot{}^{t+\Delta t}\mathbf{D}_n \\ &= \mu\,p_n\,{}^{t+\Delta t}\mathbf{n}\end{aligned} \tag{8}$$

in which $p_n$ is the penalty in contact normal direction.

Since the direction of slip varies constantly, the differentiation of ${}^{t+\Delta t}\mathbf{t}$ to $\mathbf{u}$ must be derived

$$\begin{aligned}\frac{d^{t+\Delta t}\mathbf{t}}{d\mathbf{u}} &= \frac{d}{d\mathbf{u}}\left(\frac{{}^{t+\Delta t}\mathbf{f}_t^T}{\left|{}^{t+\Delta t}\mathbf{f}_t^T\right|}\right) \\ &= \frac{{}^{t+\Delta t}\mathbf{D}_t}{\left|{}^{t+\Delta t}\mathbf{f}_t^T\right|} - {}^{t+\Delta t}\mathbf{f}_t^T\otimes\left(\frac{d}{d^{t+\Delta t}\mathbf{f}_t^T}\left(\frac{1}{\left|{}^{t+\Delta t}\mathbf{f}_t^T\right|}\right)\cdot\frac{d^{t+\Delta t}\mathbf{f}_t^T}{d\mathbf{u}}\right) \\ &= \frac{p_t}{\left|{}^{t+\Delta t}\mathbf{f}_t^T\right|}\left[\left(\mathbf{I}-{}^{t+\Delta t}\mathbf{n}\otimes{}^{t+\Delta t}\mathbf{n}\right)-{}^{t+\Delta t}\mathbf{t}\otimes\left({}^{t+\Delta t}\mathbf{t}\cdot\left(\mathbf{I}-{}^{t+\Delta t}\mathbf{n}\otimes{}^{t+\Delta t}\mathbf{n}\right)\right)\right] \\ &= \frac{p_t}{\left|{}^{t+\Delta t}\mathbf{f}_t^T\right|}\left(\mathbf{I}-{}^{t+\Delta t}\mathbf{n}\otimes{}^{t+\Delta t}\mathbf{n}-{}^{t+\Delta t}\mathbf{t}\otimes{}^{t+\Delta t}\mathbf{t}\right)\end{aligned} \tag{9}$$

where ${}^{t+\Delta t}\mathbf{f}_t^T$ is the elastic trial friction force at time $t+\Delta t$, ${}^{t+\Delta t}\mathbf{D}_t$ is the differentiation of ${}^{t+\Delta t}\mathbf{f}_t^T$ to $\mathbf{u}$ and can be written as

$${}^{t+\Delta t}\mathbf{D}_t = p_t\left(\mathbf{I}-{}^{t+\Delta t}\mathbf{n}\otimes{}^{t+\Delta t}\mathbf{n}\right) \tag{10}$$

in which $p_t$ the penalty along the contact surface, and $\mathbf{I}$ is a unit matrix. From Eq.(5), (7), (8) and (9), Eq.(4) can be finally obtained in form of

$$\begin{aligned}\frac{d^{t+\Delta t}\mathbf{f}}{d\mathbf{u}} &= \frac{p_t}{\left|{}^{t+\Delta t}\mathbf{f}_t^T\right|}\left(\mathbf{I}-{}^{t+\Delta t}\mathbf{n}\otimes{}^{t+\Delta t}\mathbf{n}-{}^{t+\Delta t}\mathbf{t}\otimes{}^{t+\Delta t}\mathbf{t}\right)+\mu\,p_n\,{}^{t+\Delta t}\mathbf{t}\otimes{}^{t+\Delta t}\mathbf{n} \\ &\quad + p_n\,{}^{t+\Delta t}\mathbf{n}\otimes{}^{t+\Delta t}\mathbf{n}-\left|{}^{t+\Delta t}\mathbf{f}_n\right|\frac{\mu_0-\mu_d}{L_d}{}^{t+\Delta t}\mathbf{t}\otimes{}^{t+\Delta t}\mathbf{t}' \\ &= \mathbf{D}^{ep}\end{aligned} \tag{11}$$

$\mathbf{D}^{ep}$ is the tangential stiffness matrix on the contact point at time t+Δt. The elastic trial is always computed at first and checked if it enters the plastic friction condition. If it is in plasticity, a return mapping procedure is triggered, as shown in Fig.5. And the state-driven $\mathbf{D}^{ep}$ will be used to replace the elastic one.

**Load increment loop: F = Δf, 2Δf, 3Δf, ...**

Initialize $\dot{u}$ $\ddot{u}$ : when **F** = 0, $\dot{\mathbf{u}}$ = 0,$\ddot{\mathbf{u}}$ = 0

when **F** = $l\Delta$**f**, $\dot{\mathbf{u}}_0^{\,l} = \dot{\mathbf{u}}^{l-1}$ , $\ddot{\mathbf{u}}_0^{\,l} = \ddot{\mathbf{u}}^{l-1}$

**Time increment loop:** $t = \Delta t, 2\Delta t, 3\Delta t, \ldots$ **until** $t_{end}$

Initialize ${}^{t}\mathbf{u}_0$, when $t = 0$, $\mathbf{u}_0 = 0$, $\lambda_0 = 0$

when $t = n\Delta t$, ${}^{t}\mathbf{u}_0 = {}^{(n-1)\Delta t}\mathbf{u}$,

**Enter Newton-raphson iteration loop:** $k = 1, 2, 3, \ldots$, **until convergence.**

Form system matrix for continuum elements

${}^{t}\mathbf{M} = \sum {}^{t}\mathbf{M}^{(e)}$, ${}^{t}\mathbf{K} = \sum {}^{t}\mathbf{K}^{(e)}$, ${}^{t}\mathbf{C} = \sum {}^{t}\mathbf{C}^{(e)}$, ${}^{t}\mathbf{Q}$

Form matrix for active contact element: Do $m = 1, 2, 3, \ldots$

if (the $m$th contact element is in contact) then

Calculate stiffness contribution ${}^{t}\mathbf{K}_c^{m}$ , assemble to ${}^{t}\mathbf{K}_c = \sum {}^{t}\mathbf{K}_c^{m}$

else

Skip to the next contact element

endif

Calculate global stiffness matrix and residual force (Subscript $d$ denotes *dynamic*).

${}^{t}\mathbf{K}_d^{k} = {}^{t}\mathbf{K} + a_0\,{}^{t}\mathbf{M} + a_1\,{}^{t}\mathbf{C} + {}^{t}\mathbf{K}_c$

Calculate the system residual:

$$\Delta\,{}^{t}\mathbf{Q}_d = {}^{t}\mathbf{Q} + {}^{t}\mathbf{M}\,[a_0\,{}^{t}\mathbf{u}_0 + a_2\,{}^{t}\dot{\mathbf{u}}_0 + a_3\,{}^{t}\ddot{\mathbf{u}}_0] + {}^{t}\mathbf{C}\,[a_1\,{}^{t}\mathbf{u}_0 + a_4\,{}^{t}\dot{\mathbf{u}}_0 + a_5\,{}^{t}\ddot{\mathbf{u}}_0] - {}^{t}\mathbf{K}_d^{k}\,{}^{t+\Delta t}\mathbf{u}_k$$

Solve displacement increments: ${}^{t}\mathbf{K}_d^{k+1}\,\Delta\mathbf{u}_{k+1} = \Delta\,{}^{t}\mathbf{Q}_d$

Update displacement: ${}^{t+\Delta t}\mathbf{u}_{k+1} = {}^{t+\Delta t}\mathbf{u}_k + \Delta\mathbf{u}_{k+1}$

Check convergence:

if( $\| {}^{t}\mathbf{Q}_d - ({}^{t}\mathbf{K} + \sum \mathbf{K}_c^{m(k)})\,{}^{t+\Delta t}\mathbf{u}_{k+1} - {}^{t}\mathbf{M}\;{}^{t}\ddot{\mathbf{u}}_0 - {}^{t}\mathbf{C}\;{}^{t}\dot{\mathbf{u}}_0 \| < tol_f$

and $\| \Delta\mathbf{u}_{k+1} \| / \| {}^{t+\Delta t}\mathbf{u}_{k+1} - {}^{t}\mathbf{u} \| < tol_d$ ) then

Update displacement, velocity and acceleration fields:

$${}^{t+\Delta t}\mathbf{u} = {}^{t+\Delta t}\mathbf{u}_{k+1}$$

$${}^{t+\Delta t}\ddot{\mathbf{u}} = a_0\left({}^{t+\Delta t}\mathbf{u} - {}^{t}\mathbf{u}_0\right) - a_2\,{}^{t}\dot{\mathbf{u}}_0 - a_3\,{}^{t}\ddot{\mathbf{u}}_0$$

$${}^{t+\Delta t}\dot{\mathbf{u}} = {}^{t}\dot{\mathbf{u}}_0 + a_6\,{}^{t}\ddot{\mathbf{u}}_0 + a_7\,{}^{t+\Delta t}\ddot{\mathbf{u}} = a_1\left({}^{t+\Delta t}\mathbf{u} - {}^{t}\mathbf{u}_0\right) - a_4\,{}^{t}\dot{\mathbf{u}}_0 - a_5\,{}^{t}\ddot{\mathbf{u}}_0$$

Exit to next time step

else

For the mid-way value ${}^{t+\Delta t}\mathbf{u}_{k+1}$, update friction force on contact surface with return mapping.

endif

**Goto next Newton-Raphson iteration**

**Goto next time step**

**Goto next load step**

Fig.6 Integration procedure of dynamic analysis with slip-weakening friction law

## 4. Numerical Integration Procedure

To investigate the dynamic response of the fault rupture process, the classical Newmark method that is one the most popular for dynamic analysis is adopted and combined with the slip weakening friction law on the fault surface. The displacement, velocity can be derived as following equations,

$${}^{t+\Delta t}\mathbf{u} = {}^{t}\mathbf{u} + {}^{t}\dot{\mathbf{u}}\,\Delta t + \frac{1}{2}\left[(1-\beta_2)\,{}^{t}\ddot{\mathbf{u}} + \beta_2\,{}^{t+\Delta t}\ddot{\mathbf{u}}\right]\Delta t^2 \qquad (12.1)$$

$${}^{t+\Delta t}\dot{\mathbf{u}} = {}^{t}\dot{\mathbf{u}} + \left[(1-\beta_1)\,{}^{t}\ddot{\mathbf{u}} + \beta_1\,{}^{t+\Delta t}\ddot{\mathbf{u}}\right]\Delta t \qquad (12.2)$$

where $\Delta t$ is the time increment, superscript $t+\Delta t$ and $t$ denote time steps, and $\beta_1$ and $\beta_2$ are two Newmark parameters. In our case, $\beta_2$=0.5, $\beta_1$ =0.25 are for the implicit integration algorithm.

The standard formulation of Newmark method can be referred to the Finite Element Method [9]. By considering the discontinuity on fault surface, the dynamic equation evolves to

$$\mathbf{M}\,{}^{t+\Delta t}\ddot{\mathbf{u}} + \mathbf{C}\,{}^{t+\Delta t}\dot{\mathbf{u}} + \mathbf{K}\,{}^{t+\Delta t}\mathbf{u} + {}^{t+\Delta t}\mathbf{K}_c\,{}^{t+\Delta t}\mathbf{u} = {}^{t+\Delta t}\mathbf{Q} \qquad (13)$$

in which **M**, **C** and **K** are mass, damping and stiffness

matrix respectively for continuum that are considered not to change with the variation of time, ${}^{t+\Delta t}\mathbf{Q}$ is the external force, while ${}^{t+\Delta t}\mathbf{K}_c$ is the stiffness matrix of master-slave contact elements on the fault.

By substituting equation(12.1) and (12.2) into (13), it obtains the equation to calculate ${}^{t+\Delta t}\mathbf{u}$ from ${}^{t}\mathbf{u}$, ${}^{t}\dot{\mathbf{u}}$ and ${}^{t}\ddot{\mathbf{u}}$

$$\begin{aligned}&(\mathbf{K}+a_0\mathbf{M}+a_1\mathbf{C}+{}^{t+\Delta t}\mathbf{K}_c)\,{}^{t+\Delta t}\mathbf{u}\\&={}^{t+\Delta t}\mathbf{Q}+\left[a_0\,{}^{t}\mathbf{u}+a_2\,{}^{t}\dot{\mathbf{u}}+a_3\,{}^{t}\ddot{\mathbf{u}}\right]\mathbf{M}\\&\quad+\left[a_1\,{}^{t}\mathbf{u}+a_4\,{}^{t}\dot{\mathbf{u}}+a_5\,{}^{t}\ddot{\mathbf{u}}\right]\mathbf{C}\end{aligned}\qquad(14)$$

where $a_0$ to $a_5$ are parameters that depend on $\beta_1$, $\beta_2$ and time increment $\Delta t$.

$$a_0=\frac{1}{\beta_1\Delta t^2},\quad a_1=\frac{\beta_2}{\beta_1\Delta t},\quad a_2=\frac{1}{\beta_1\Delta t}$$

$$a_3=\frac{1}{2\beta_1}-1,\ a_4=\frac{\beta_2}{\beta_1}-1,\quad a_5=\frac{\Delta t}{2}\left(\frac{\beta_2}{\beta_1}-2\right)\qquad(15)$$

The integration procedure of dynamic analysis with slip weakening friction law can be described in Fig.6. The dynamic displacement solution at a given time is applied to the contact surface to calculate the relative slip and friction force, following the proposed slip-weakening friction law. This dynamic model has been implemented into GeoFEM [10], a parallel finite element code developed by RIST members for purpose of very large simulation of the crust motion.

## 5. Simulation of Fault Dynamic Rupture of Northeast Japan

The earthquake generation consists of two processes: a long time of friction force accumulation at some certain bonded zones on the fault surface due to gravity and the constant relative shift between plates; and an instantaneous rupture of the bonded zones that leads to the occurrence of earthquake. Usually, the first process takes from several years to even over hundreds of years, while second one only lasts a few seconds.

In Northeast Japan, there spread many bonded zones on the fault surface, as shown in Fig.7, where the friction force is accumulated, while the rest of the fault has already been in the shifting status. A higher

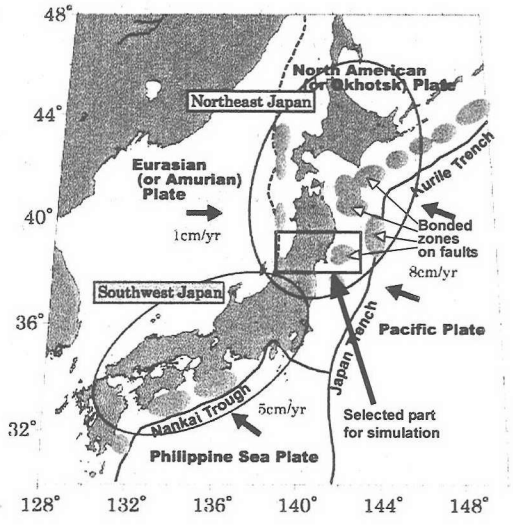


Fig.7 Fault location around Japan Island

friction coefficient at the bonded zones than the other area on the fault is considered as one of the reasons that cause the different statuses between them.

A rectangle area in Northeast Japan, marked in Fig.7, with 620km long (west-east), 200km wide (north-south) and 200km deep, is selected to perform the simulation. The simulation model includes the upper most crust, the mantle beneath and the shifting plate. Between the mantle and the plate is the fault with an inclined angle of $28.5^0$(see Fig.8).

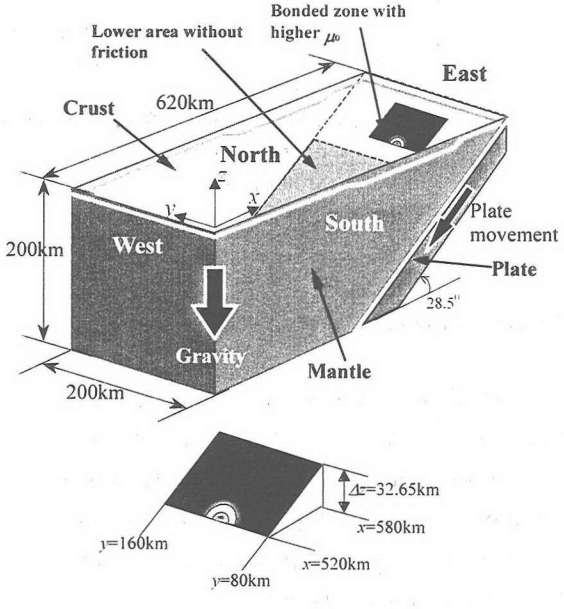


Fig.8 Geometry of selected part of Northeast Japan for FE simulation

Table 1 Material properties of crust, mantle and plate

| | Young's modulus ($N/m^2$) | Poisson ratio | Density ($Kg/m^3$) |
|---|---|---|---|
| Crust | $2.69\times10^7$ | 0.226 | $2.7\times10^3$ |
| Mantle | $3.82\times10^7$ | 0.273 | $3.3\times10^3$ |
| Plate | $12.07\times10^7$ | 0.258 | $3.0\times10^3$ |

Table 2 Fault properties for simulation

| Penalty Number | Dynamic friction coefficient $\mu_d$ | Slip-weakening distance $L_d$(m) |
|---|---|---|
| $5.0.\times10^{11}$ | 0.6 | 1.0 |

The selected part is discretized by hexahedral elements for the mantle, crust and plate respectively, and by master-slave contact element for the inclined fault between mantle and plate. The mesh size of hexahedral element is about 2.5×2.5×2.5km, thus over 2,300,000 finite element nodes are generated. Mantle and crust are connected without specified surface. They are only different in material properties. The material properties of crust, mantle, plate and fault are list in Table 1.

On the fault surface, a dark color area indicates the bonded zone, where the friction force is accumulated until it ruptures. As addressed previously, it is assumed that the bonded zone has higher friction coefficient than the other area to hold the accumulated friction force. Herein, it is set to $\mu_0$=0.606 that is 1.00% higher than the dynamic friction coefficient $\mu_d$=0.6. When the friction force at a certain location on the bonded zone reaches the shear strength the equilibrium is broken suddenly, from which the rupture begins to propagate rapidly through the whole bonded zone. The friction coefficient of any point on the bonded zone would decrease from $\mu_0$ to $\mu_d$, following the slip-weakening law. With the increasing depth, the mantle gradually changes from solid phase to approximately fluid due to the increasing temperature. For simplification, the present simulation assumes the friction on the fault surface deeper than 60km is ignored. Because it is deeper than lower boundary of bonded zone, this simplification assuming the friction discontinuity is considered not to have significant influence on the fault dynamic rupture process. Table 2 gives the fault properties used in simulation. A large value of penalty number is chosen to prevent the contact node from penetrating into the contact surface. For slip-weaken

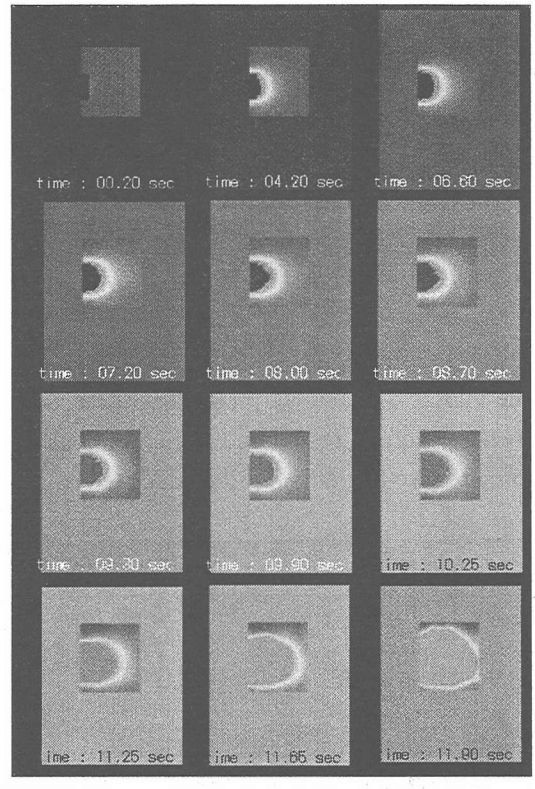


Fig.9 friction coefficient variation on bonded zone in dynamic analysis

-ing distance $L_d$, since there is not yet unified data for real fault, it is set as 1.0m, referred to the report by Guatteri and Spudich [11].

The fixed boundary are as follows: the west sides of mantle and crust in X direction, the north and south sides of mantle, crust and plate in Y direction, and the bottom of mantle in Z direction. The displacement boundary, as an input force, is assigned to the plate along the fault surface with a constant velocity during the force accumulation process, which is calculated from the observation shift velocity of Pacific and Eurasian plates(see Fig.7), following the formula

$$\dot{u}_b = (8\text{cm/ys}+1\text{cm/ys})\times\cos(28.5^0) = 2.508\times10^{-9}\text{m/sec} \quad (16)$$

The loading procedure is divided into two steps. In the first step, the gravity force of crust and mantle is acted, creating the normal pressure on the fault surface. Simultaneously, the motion of plate with rate $\dot{u}_b$ is assigned to have friction force accumulate on bonded zone, and have the other area on fault be in

frictional slipping status. This is thought as a quasi-static process. In the second step, the dynamic analysis is triggered when the bond zone begins to break. An initial slip velocity and acceleration at the beginning of the dynamic analysis is assumed by enforcing a 4m slip over 0.1sec. It is found that the rupture always initiates at lower boundary of the bonded zone, and usually it occurs from a small region, where is physically imperfect, then propagates widely. To approximate such a possible imperfection in reality, we specify a 20km×5km weaker region near the middle of the lower boundary of the bonded zone, where a quick reduction of friction coefficient is enforced at the beginning of dynamic analysis.

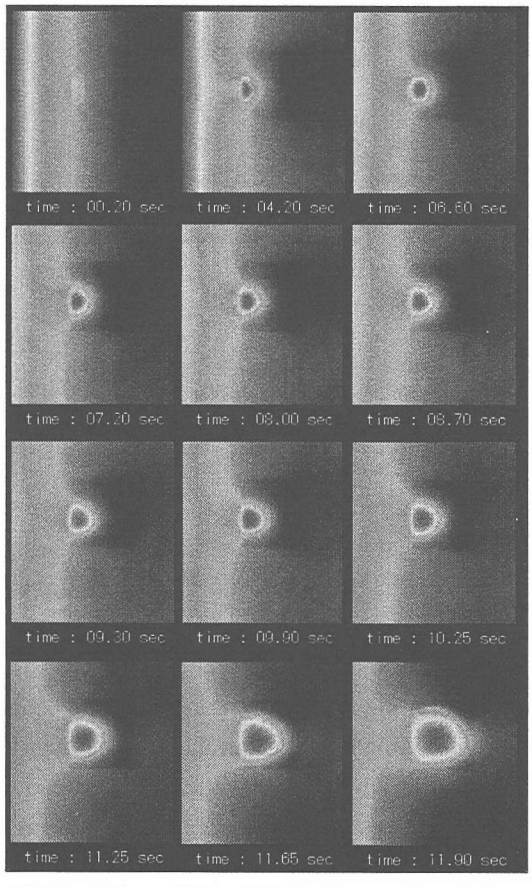


Fig.10 Variation of slip distribution on bonded zone

The simulation is carried out on the vectorized parallel supercomputer-Earth Simulator [9], by 16 computing nodes of totally 128 processors. The time increment for each time step is in the range from 0.1~0.2sec that is considered small enough for stable dynamic integration. Totally 80 steps are performed, which costs 2 hour computing time.

The simulation results of $\mu$ and slip distributions with variation of time are shown in Fig.9 and Fig.10 respectively. From Fig.9, the friction coefficient of the bonded zone decreases and eventually drops to the same level of other area that has been in shift. In this process, a huge energy stored during friction force accumulation is released in a short of time, thus generating the earthquake wave to the surface of the earth. The slip-distribution in Fig.10 shows that the ruptured region on the bonded zone has a larger slip in the dynamic rupture process. Its distribution is consistent with that of slip in Fig.9.

Both figures represent that the fault rupture develops slowly up to time=10sec and thereafter speeds up to the whole patch area. This explains that the dynamic rupture, at the occurrence, propagates relatively stable because the fault can still bear friction force. With the expansion of the ruptured area, the stiffness of the bonded zone reduced rapidly, and the rupture propagation speeds up until the complete breakdown of the bonded zone. This basically reflects the dynamic rupture process at the initial stage of earthquake.

## 6. Conclusions

By implementing the slip-weakening friction law into GeoFEM code, large scale simulation of dynamic fault rupture in selected part of Northeast Japan is achieved.

It is seen that the slip-weakening friction law adopted in the present study, though being simple, is considered to be basically applicable to describe the fault rupture behavior. More importantly, a large-scale finite element simulation of fault dynamic rupture has been realized on Earth Simulator, and the simulation result qualitatively reflects the instantaneous rupture process at the initial stage of earthquake. However, in this simulation case, some simplifications are assumed, such as plane shape of the fault surface, no geometry dependence on fault properties, etc. Therefore, to improve the accuracy and reliability of the simulation for earthquake prediction, more intensive work should be continued in both the fault friction modeling and the complexity of fault geometry.

**Acknowledgement**

The financial support from Science and Technology Promotion Funds for Earth Simulator Project by the Ministry of Education, Culture, Sport, Science and Technology is gratefully acknowledged.

**References**

1) http://www.es.jamstec.go.jp
2) Dieterich, J.H.: A model for the nucleation of earthquake slip, in *Earthquake Source Mechanics, Geophysical Monograph*, eds Das, S., Boatwright, J. & Scholmz, C.H., AGU, Washington, DC, Vol.37, Maurice Ewing Ser. 8, pp.37-47, 1986.
3) Prabhakar, G. and Iizuka, M.: New method for the integration of fault constitutive equations, 3rd ACES International Workshop, Maui, 2002.
4) 久田俊明，野口裕久：非線形有限要素法の基礎と応用，丸善，1995
5) Andrews, D.J.: Rupture propagation with finite stress in antiplane strain, *J. geophys. Res.*, Vol.81, pp.3575-3582, 1976.
6) Ohnaka, M. & Yamashita, T.: A cohesive zone model for dynamic shear faulting based on experimentally inferred constitutive relation and strong motion source parameters, *J. geophys. Res.*, 94, pp.4089-4104, 1989.
7) 坪井利弘，三浦房紀：断層運動を模擬する岩石すべり破壊実験の有限要素解析，土木学会論文集 No.537/I-35，pp.61-76，1996.
8) Peric, D. & Owen, R.J.: Computational model for 3-D contact problems with friction based on the penalty method, *Int. J. numerical method in eng.*, Vol.35, pp.1289-1309, 1992.
9) Zienkiewicz, O.C. and Taylor, R.L: The finite element method, fifth edition, Vol.1 The basic, Butterworth Hernemann, 2002.
10)http://www.tokyo.rist.or.jp/Geofem
11)Guatteri, M. and Spudich, P.: What can strong motion data tell us about slip-weakening friction laws? http://pangea.stanford.edu/~patti/BSSA_99

(Received April 18,2003)